

Numerical and experimental investigation of HDPE behavior during 2-ECAP process using 90° and 120° dies

Ali Mitsak¹ · Benaoumeur Aour¹

Received: 5 September 2015 / Accepted: 15 May 2016 / Published online: 10 June 2016
© The Brazilian Society of Mechanical Sciences and Engineering 2016

Abstract Among various severe plastic deformation methods, equal channel angular pressing (ECAP) is an effective tool to introduce large plastic deformation of simple shear. The principle consists to extrude the sample several times through two intersecting channels with the aim to improve the mechanical properties of the material by altering the morphology of its microstructure. In this work, a numerical and experimental investigation of a typical semi-crystalline thermoplastic polymer (high density polyethylene, HDPE) during two-turn ECAP (2-ECAP) using 90° and 120° dies has been presented. The warping of the extruded samples has been also highlighted experimentally. The material parameters of an elasto-viscoplastic constitutive law were identified using compressive tests at different temperatures and strain rates. The effects of the main parameters, such as, the channel angles, the dimensions of the intermediate channel, the friction and the temperature have been analyzed. Finally, to confirm the numerical results, two dies composed of one elbow (1-ECAP) and two elbows (2-ECAP) have been manufactured and tested. It was found that the warping obtained using 2-ECAP die is more reduced than that of 1-ECAP die even with several passes.

Keywords ECAP · HDPE · Finite element · Temperature · Friction

Technical Editor: Márcio Bacci da Silva.

✉ Benaoumeur Aour
ben_aour@yahoo.fr

Ali Mitsak
ali_mitsak@yahoo.fr

¹ Laboratory of Applied Biomechanics and Biomaterials,
National Polytechnic School of Oran, BP1523 EL M'naour,
31000 Oran, Algeria

1 Introduction

Equal channel angular pressing (ECAP) is an effective tool to impose large plastic strains. The process, developed first by Segal et al. [1], has attracted considerable interest as a method to improve the material properties by super plastic deformation. Indeed, this process involves simple shear deformation that is achieved by pressing the work piece through a die containing two channels of equal cross-section that meet at a predefined angle. This method has been proved to be very effective in producing ultrafine grain size in metallic materials [2–4] and a significant molecular orientation in the case of polymeric materials [5–16] with accompanying enhancement in mechanical properties.

According to our knowledge, this process was first applied to polymers by Sue and Li [5]. They showed that the ECAP process is efficient in altering the morphology of a linear low density polyethylene (LLDP). Sue et al. [6] have been reported that for ECAP to be effective, it is necessary that the extrusion be held at temperatures slightly below the glassy transition in the case of polycarbonate (PC). For the same polymer, Li et al. [7] confirmed that the mechanical properties can be tailored by extruding the material via various processing routes and different number of passes. The effect of molecular anisotropy on the impact strength of polycarbonate (PC) was examined by Xia et al. [8]. They found that the enhancement of the impact resistance is directly related to the changes in molecular orientation induced by ECAP process. According to Xia et al. [9], the crystallinity and molecular orientation have been identified as two important factors affecting the dynamic mechanical properties of the ECAP-oriented semi-crystalline polyethylene terephthalate (PET). An improvement of bending and torsional storage modulus was found. Creasy

and Kang [10] studied fiber fracture during ECAP process of short fiber-reinforced thermoplastics. They found that the fiber length can be controlled and oriented by setting the process temperature below the melting point of the polymer crystallites. On the other hand, the effect of different ECAP routes on the tensile, fracture toughness, flexural and ballistic impact properties of polymethyl methacrylate (PMMA) was investigated by Weon et al. [11]. The process was also used to modify the aspect ratio and orientation of clay nanoparticles in nylon-6/clay nanocomposites by Weon and Sue [12]. A fruitful discussion was reported by Wang et al. [13] on lamellar formation and relaxation in simple sheared polyethylene terephthalate (PET) using the in situ time resolved synchrotron small-angle x-ray scattering (SAXS) technique. More recently, numerical and experimental investigations were achieved to highlight the effects of the main geometrical and processing parameters on the viscoplastic behavior of polymers during ECAP process [14–16].

ECAP impact on microstructure and on the enhancement of mechanical and physical properties of polymers reported in the very few investigations available in the literature support the effectiveness of this process for polymeric materials. However, up to now, the majority of investigations have been conducted on 1-ECAP die. To improve the level of the plastic strain (with a good homogeneity) and reduce the significant curvature of the 1-ECAP extruded samples of polymers [6, 17], an optimization of the die geometry composed of two elbows has been investigated. The general principle of 2-ECAP process is shown in Fig. 1. The tool is a block containing three intersecting equal cross-section channels. A sample which is placed into the entrance channel is extruded through the exit channel by a punch. Under these conditions, the sample passes by two elbows in one pass. The respective effects of the processing parameters, such as, the die geometry and the processing conditions on the plastic strain distribution and the evolution of the pressing force have been highlighted using 90° and 120° dies.

It is worth noting that the major motivation of this work is to investigate the behavior of a high density polyethylene using 2-ECAP to improve the level and the homogeneity of the plastic strain and to highlight the reduction of the sample warping. To achieve this objective, the paper was organized as follows. The elasto-viscoplastic constitutive law and its identification using compressive tests at different strain rates and different temperatures are presented, respectively, in Sects. 2 and 3. Section 4 introduces details on the finite element modeling. The numerical results obtained for the effects of friction and temperature on the plastic strain distribution and the evolution of the pressing force using two dies of 90° and 120° are presented in Sect. 5. Section 6 gives a comparison between the experimental results

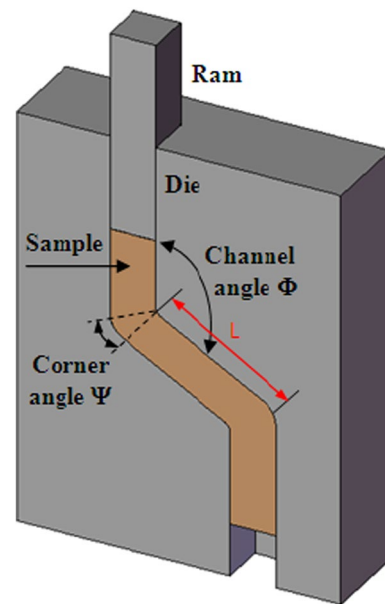


Fig. 1 Schematic illustration of two-turn equal channel angular pressing process

obtained using 1-ECAP and 2-ECAP dies. Finally, Sect. 7 gives the main remarks.

2 Constitutive model

The large plastic deformation of the polymer under study (HDPE) is characterized by a strain rate dependent yield followed by a strain hardening. Various constitutive laws, basing on micromechanical or phenomenological considerations [18, 19], were developed to describe the specific behavior of polymers. In this paper, a phenomenological constitutive model was used to describe the behavior of the studied material [20]. It is based on the additive decomposition of the strain rate tensor \mathbf{d} into an elastic part \mathbf{d}^e and a viscoplastic part \mathbf{d}^{vp} as:

$$\mathbf{d} = \mathbf{d}^e + \mathbf{d}^{vp} \quad (1)$$

The elastic strain rate tensor \mathbf{d}^e is given by:

$$\mathbf{d}^e = \mathbf{C}^{-1} \tilde{\sigma} \quad (2)$$

$$\tilde{\sigma} = \dot{\sigma} - \mathbf{W}\sigma + \sigma\mathbf{W} \quad (3)$$

where $\tilde{\sigma}$ the Jaumann derivative of the Cauchy stress tensor is σ based upon the spin tensor \mathbf{W} and \mathbf{C} is the fourth-order isotropic elastic modulus tensor:

$$C_{ijkl} = \frac{E}{2(1+\nu)} \left[(\delta_{ik}\delta_{jl} + \delta_{il}\delta_{jk}) + \frac{2\nu}{1-2\nu} \delta_{ij}\delta_{kl} \right] \quad (4)$$

where E , ν and δ are the Young’s modulus, Poisson’s ratio and Kronecker-delta symbol, respectively.

The viscoplastic strain rate tensor \mathbf{d}^{vp} can be expressed by the following relationships:

$$\mathbf{d}^{vp} = \frac{3}{2} \left\langle \frac{\sigma_e - R}{K} \right\rangle^n \frac{\sigma'}{\sigma_e} \quad (5)$$

$$\sigma' = \sigma - tr(\sigma)/3\mathbf{I} \quad (6)$$

$$\sigma_e = \sqrt{3/2\sigma'\sigma'} \quad (7)$$

where K and n are the viscosity parameters, σ' is the deviator stress tensor, σ_e is the equivalent stress, and R is the isotropic hardening defined by a simple phenomenological evolution law as follows:

$$R = h \left(1 + \frac{\varepsilon^p}{\varepsilon_0} \right)^m \quad (8)$$

$$\varepsilon^p = \int_0^t \dot{\varepsilon}^p d\tau = \int_0^t \sqrt{2/3\mathbf{d}^{vp}\mathbf{d}^{vp}} d\tau \quad (9)$$

with ε^p is the equivalent viscoplastic strain, ε_0 is the initial yield strain, m and h are the hardening parameters.

3 Fitting experimental data

To simulate the plastic flow behavior of HDPE during 2-ECAP process, using finite element analysis, a series of compressive tests on HDPE specimens were carried out to identify the parameters of the elasto-viscoplastic constitutive law presented in the previous section. The HDPE material was provided by Goodfellow© company as a cylindrical bar of 10 mm diameter and length of 1000 mm, with a number-average molecular weight $M_n = 10 \text{ kg mol}^{-1}$ and a weight-average molecular weight $M_w = 70 \text{ kg mol}^{-1}$. The percentage of crystallinity is approximately 70 % with a specific gravity of 0.95 g/cm³. To conduct compressive tests, cylindrical specimens of 10 mm diameter and 20 mm height were cut according to the longitudinal direction of the bar using an automatic machine tool. It was noted that a particular attention was taken during the realization of the specimens for obtaining the flat parallel surfaces, and simultaneously perpendicular to the long axis of the specimen. The machined facets were also polished. To eliminate the residual stress due to processing and machining, the specimens were heat-treated in an oven at a temperature of 90 °C for 18 h and then cooled down to room temperature for few days before testing. The experimental

tests were performed on an electromechanical testing machine (Instron® 5800) with a load-cell of 10 kN at different temperatures ($T = 25, 40, 60$ and 80 °C) and strain rates ($10^{-2}, 10^{-3}$ and 10^{-4} s^{-1}). It was also noted that the plates of the testing machine were well lubricated, so that the friction effect at the contact surfaces with the specimen is negligible. During tests, the values of crosshead displacement, force and time were recorded by the computer using Bluehill software. The experimental stress–strain curves obtained from compressive tests on HDPE are shown in Fig. 2. Compression strain and stress are plotted as positive values. It can be seen that the mechanical response of HDPE is nonlinear with an evident transition from elastic to inelastic stage.

The constitutive equations introduced in Sect. 2 were used to predict the nonlinear behavior of HDPE at large strains. In addition to the Young’s modulus and Poisson’s ratio, the constitutive equations contain four parameters to be determined: K , n , m and h . They were identified using a least squares regression fitting method. The Young’s modulus E was deduced from the slope of the initial linear portion of the compression stress–strain curve. The Poisson’s ratio ν was taken equal to 0.38. Table 1 gives the values of the identified material parameters. Figure 2 gives the comparison between the experimental data (in symbols) and the elasto-viscoplastic constitutive model (in solid lines) for HDPE at 25 °C (Fig. 2a), 40 °C (Fig. 2b), 60 °C (Fig. 2c) and 80 °C (Fig. 2d). It can be seen that a fairly good agreement is obtained between the experimental data and the theoretical constitutive elasto-viscoplastic law.

It is recognized that the constitutive law parameters were identified using data compression at different strain rates while the ECAP process generally induces plastic deformation strongly anisotropic and complex. Indeed, this model represents a simple approach to optimize the geometrical and operating parameters of the process before taking into account the multiaxiality of the deformation. It should be noted that this identification was also used to optimize 1-ECAP process which induces also complex plastic deformation mechanisms [20–22]. Perhaps, progressive deformation multiaxial with uniaxial identification was adopted by several authors [23, 24]. Moreover, the identification and quantification of the plastic anisotropy has a very special interest for super plastic deformation process. However, it is planned to validate the model on other types of multiaxial loading to improve the prediction of behavior, but it is more interesting to develop a multiscale model that takes into account the evolution of microstructure in combination with macroscopic behavior of the processed material. In this case, the parameter identification will be more realistic after the completion of the experimental device which will be specifically developed and this is the object for a future work.

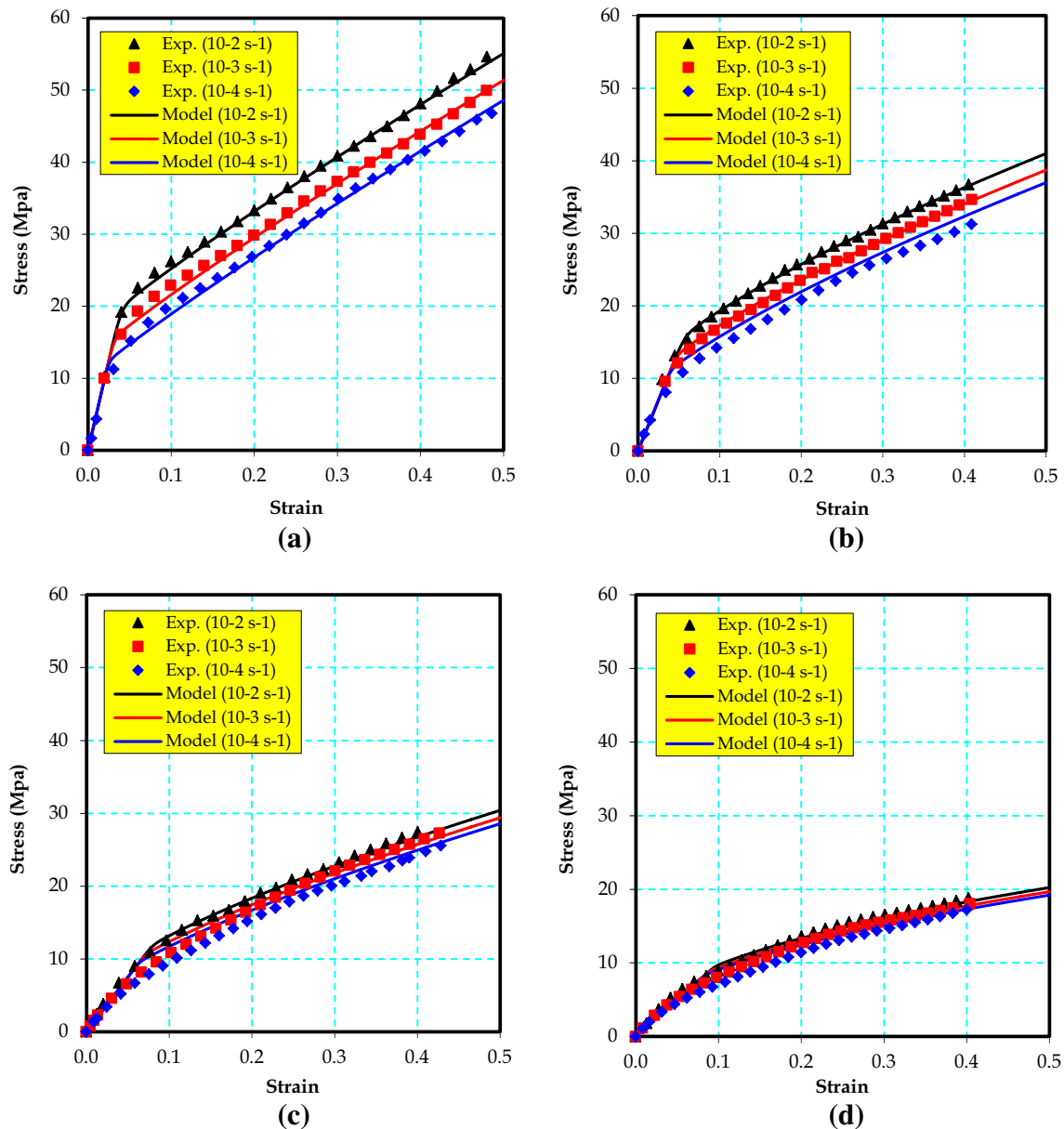


Fig. 2 Stress-strain curves of HDPE for various temperatures: **a** room temperature (25 °C); **b** 40 °C, **c** 60 °C; **d** 80 °C

Table 1 The material parameters for HDPE at different temperatures

T (°C)	E (Mpa)	K (Mpa)	N (–)	H (Mpa)	M (–)
25	500	31.2	7.8	3.15	0.88
40	280	20	8.3	5	0.7
60	150	10.7	10.2	5.5	0.65
80	130	5.7	11.17	6	0.45

4 Finite element modeling

The simulations were carried out using the finite element software MSC.Marc under plane-strain conditions. The

sample dimensions were 10 mm (width) \times 10 mm (thickness) \times 110 mm (length). Initially, the die geometry was taken with channel angle $\Phi_1 = \Phi_2 = \Phi = 90^\circ$ (and 120°) and the two outer corners angles have been fixed to 10° . A radii $r = 2$ mm has been taken at the inner corners. It was noted that these values have been selected according to the previous study undertaken by Aour et al. [22]. Initially, the friction coefficient between the sample and the die channels was assumed to be zero, implying frictionless condition (for the first tests).

The die and the ram were considered as rigid bodies in the modeling. A displacement of 110 mm was assigned to the ram in the extrusion direction. According to the

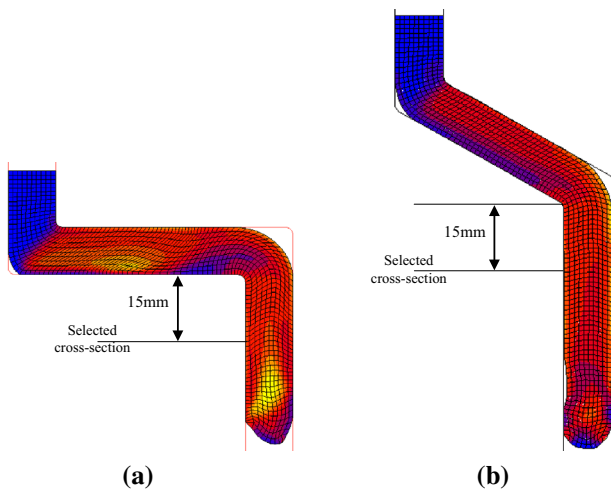


Fig. 3 Illustration of the finite element meshes of the samples and the selected cross-section for the measurement in the case of: **a** 90° die and **b** 120° die

theoretical [4] and experimental [25] analysis, the isothermal condition can be fulfilled at low pressing speeds. So, all simulations were performed with a ram speed of 0.1 mm/s, which generates negligible heat due to the plastic deformation [22]. The sample behavior was considered as being elasto-viscoplastic. To control the plastic strain distribution, the selected cross-section was taken at 15 mm below the second inner corner (see Fig. 3).

5 Results and discussion

5.1 Equivalent plastic strain distribution

In ECAP process, the homogeneity of the plastic strain distribution in the bulk material during successive passes is very important. The aim of this section is to determine the optimal conditions which allow us to improve the homogeneity of the plastic strain distribution in terms of the

thickness (t) and the length (L) of the second channel for the two-elbow tool.

5.1.1 Case of 90° die

Figure 4 shows the equivalent plastic strain distribution for four different lengths $L = \{20, 30, 40 \text{ and } 50 \text{ mm}\}$ with a section of $w \times t = 10 \times 10 \text{ mm}^2$ and an inner corner radii of 2 mm. It can be observed that the plastic strain is not uniform at the end of the samples. However, at the middle, the homogeneity of the plastic strain distribution is relatively improved, especially after the second pass except in the case of $L = 20 \text{ mm}$. This is due to the phenomenon of folding which is much more pronounced when the second channel length is low ($L = 20 \text{ mm}$).

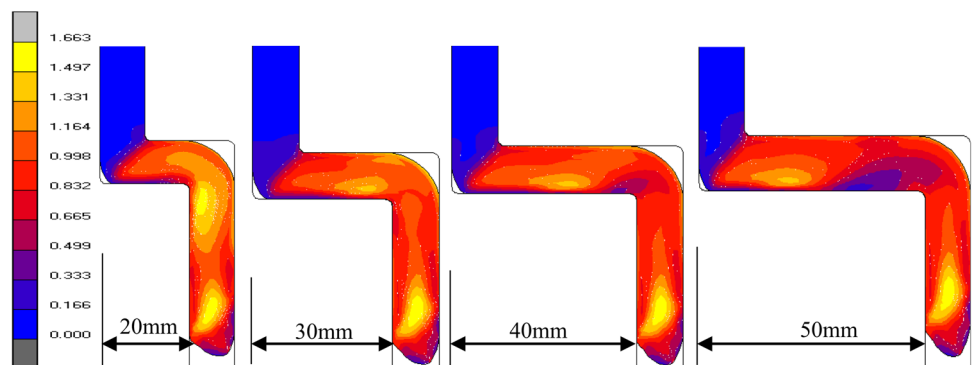
For more details, we have shown in Fig. 5 the distribution of the equivalent plastic strain in terms of distance from the bottom along the selected cross-section of the sample (see Fig. 3) for each thickness with different lengths of the second channel. It can be seen that the low equivalent plastic strain is obtained when the length $L = 50 \text{ mm}$ for all cases. However, the high level of plastic strain is obtained when the length $L = 30 \text{ mm}$ for $t = 8, 10$ and 12 mm while for $t = 6 \text{ mm}$ the high level of plastic strain is obtained when the length $L = 40 \text{ mm}$.

It is worth noting that the variation factor is an important parameter, which can be related to the strain homogeneity (i.e., the higher its value, the more important is the heterogeneity of the deformation) [21]. So, to quantify the degree of the plastic strain homogeneity, a statistical analysis has been carried out by introducing the standard deviation and the variation factor V , defined as the ratio of the standard deviation to the average strain as

$$V = \frac{1}{\varepsilon_{ave}} \sqrt{\frac{1}{N} \sum_{i=1}^N (\varepsilon_i - \varepsilon_{ave})^2} \times 100 (\%) \quad (10)$$

where ε_i is the equivalent plastic strain value of a given integration point along the sample width, ε_{ave} is the arithmetic

Fig. 4 Equivalent plastic strain contours for HDPE samples during 2-ECAP process using 90° die for different lengths of the second channel



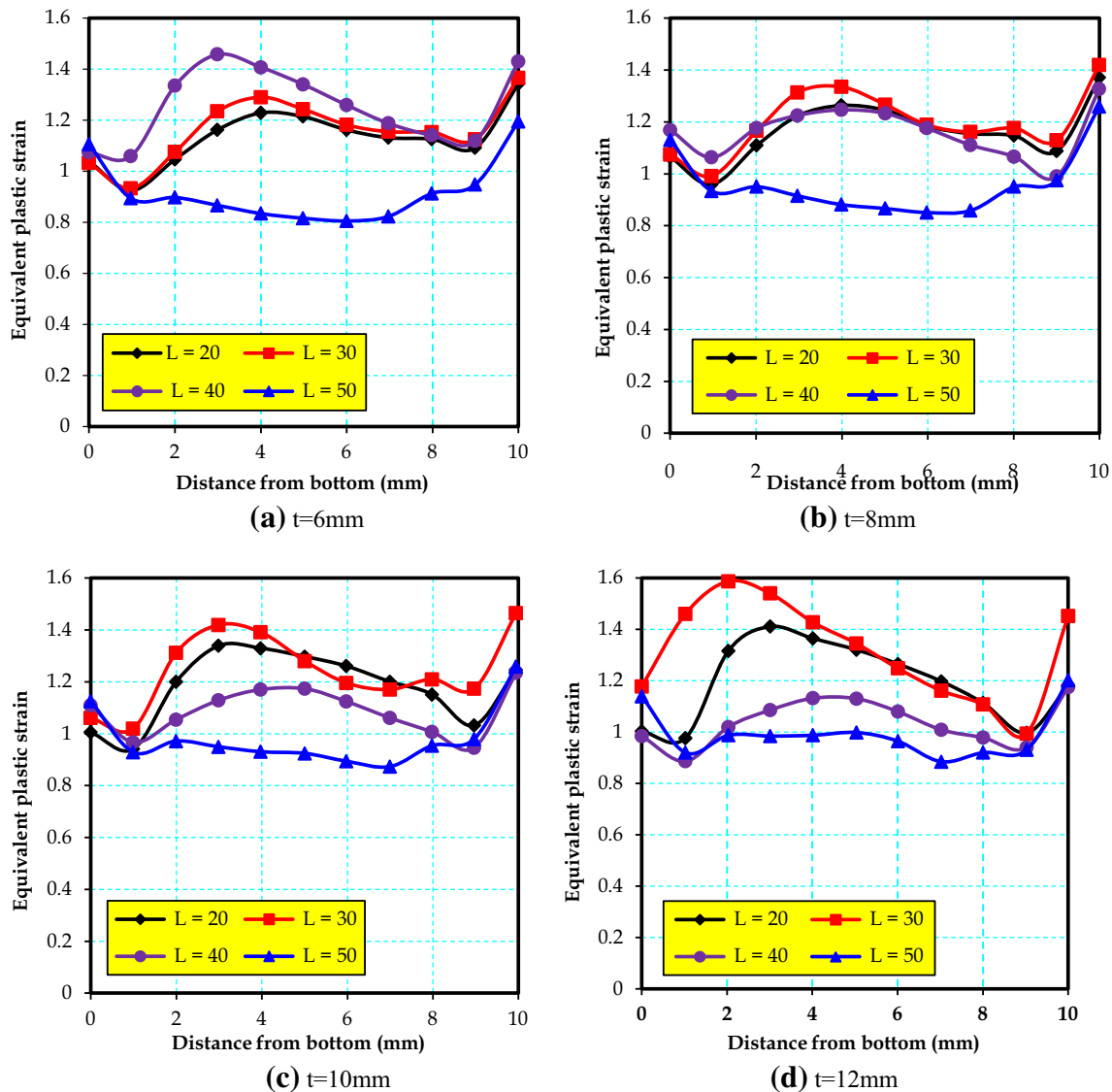


Fig. 5 Distribution of the equivalent plastic strain along the selected cross-section for different lengths and thicknesses of the second channel in the case of 90° die

average of the equivalent plastic strain values computed on N integration points.

The maximum punch force required, and the maximum and the average values of the equivalent plastic strain given by the numerical solution as well as the variation factor and the standard deviation calculated according to the different geometries are presented in Table 2. It can be remarked that the maximum punch force increases with the increase of the second channel thickness. Nonetheless, the average plastic strain varies from 0.926 to 1.320 for all cases. However, by considering the variation factor, it can be concluded that the best homogeneity of the plastic strain distribution was obtained when the thickness $t = 10$ mm and the length $L = 40$ mm. Moreover, one can note that the more

heterogeneous plastic deformation is obtained with a thickness of 12 mm and a length of 30 mm.

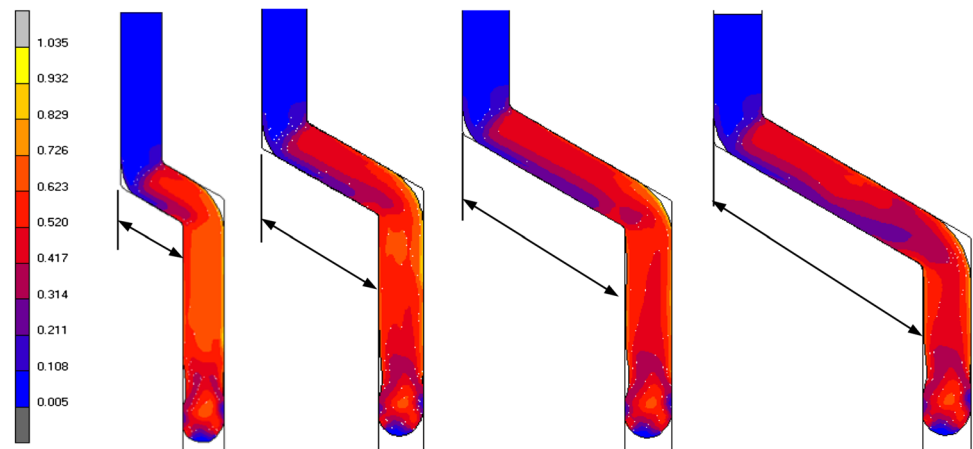
5.1.2 Case of 120° die

The same simulations have been carried out for the case of 120° die and the obtained results are depicted in Fig. 6. It can be seen that the equivalent plastic strain distribution is relatively uniform and homogeneous compared to that of 90° die. To give more details, we presented in Fig. 7 the evolution of the equivalent plastic strain in terms of distance from the bottom along the selected cross-section of the sample for each thickness with different lengths of the second channel. It can be observed that the low equivalent

Table 2 Evolution of the punch force, the equivalent plastic strain and the variation factor in terms of t and L in the case of 90° die

Thickness t (mm)	L (mm)	Maximum punch force required (kN)	Maximum strain	Average strain	Standard deviation	Variation factor (%)
6	20	9.675	1.348	1.138	0.106	9.285
	30	9.512	1.367	1.166	0.116	9.980
	40	9.675	1.465	1.259	0.143	11.340
	50	9.747	1.204	0.926	0.121	13.069
8	20	12.765	1.371	1.173	0.105	8.948
	30	12.710	1.427	1.208	0.117	9.712
	40	12.700	1.316	1.167	0.093	7.962
	50	12.710	1.268	0.970	0.121	12.467
10	20	15.697	1.343	1.187	0.129	10.903
	30	15.810	1.470	1.251	0.136	10.891
	40	15.724	1.244	1.093	0.087	7.923
	50	15.794	1.274	0.989	0.110	11.164
12	20	17.855	1.411	1.197	0.148	12.356
	30	19.073	1.593	1.320	0.183	13.881
	40	18.938	1.180	1.040	0.087	8.333
	50	19.008	1.217	0.999	0.095	9.478

Fig. 6 Equivalent plastic strain contours for HDPE samples during 2-ECAP process using 120° die for different lengths of the second channel



plastic strain is obtained when the length $L = 50$ mm for all cases. However, the high level of plastic strain is obtained when the length $L = 20$ mm and $t = 10$ or 12 mm while when $t = 6$ and 8 mm the high level of plastic strain is obtained when the length $L = 30$ mm.

Table 3 shows the values of the maximum punch force required, and the maximum and the average values of the equivalent plastic stain given by the numerical solution as well as the variation factor and the standard deviation calculated according to the different geometries in the case of 120° die. It can be observed that the maximum punch force decreases with the decrease of the second channel thickness. Furthermore, the limits of the average plastic strain varies from 0.581 (at $t = 6$ mm and $L = 50$ mm) to 0.675 (at $t = 10$ mm and $L = 20$ mm) for all the presented cases.

By taking into account the variation factor criterion, it can be deduced that the best homogeneity of the plastic strain distribution was obtained when the thickness $t = 10$ mm and the length $L = 20$ mm.

5.2 Evolution of the pressing force

The magnitude and the distribution of the plastic strain in the sample can be seen as key parameters for the ECAP process. While the magnitude of the pressing force required to extrude the sample, defined the practical limit of the ECAP device. The numerical results of the pressing force required for HDPE extrusion was calculated from the nodal forces at the top of the sample. The evolution of this force as a function of the time in Fig. 8 for a cross-section of 10×10 mm²

Fig. 7 Distribution of the equivalent plastic strain along the selected cross-section for different lengths and thicknesses of the second channel in the case of 120° die

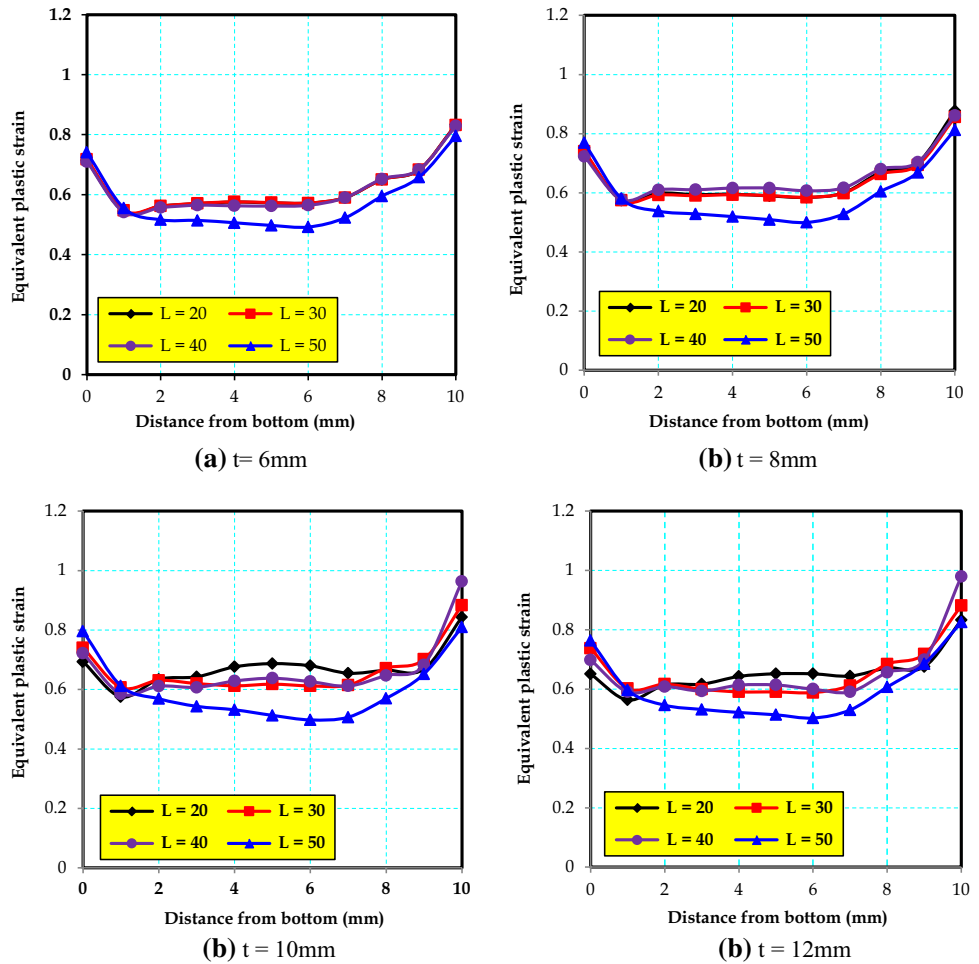


Table 3 Evolution of the punch force, the equivalent plastic strain and the variation factor in terms of t and L in the case of 120° die

Thickness t (mm)	L (mm)	Maximum punch force required (kN)	Maximum strain	Average strain	Standard deviation	Variation factor (%)
6	20	2.575	0.833	0.624	0.084	13.502
	30	2.618	0.832	0.625	0.084	13.421
	40	2.683	0.829	0.620	0.086	13.824
	50	2.624	0.796	0.581	0.100	17.280
8	20	3.651	0.877	0.647	0.089	13.763
	30	3.590	0.856	0.643	0.084	13.126
	40	3.612	0.861	0.656	0.078	11.899
	50	3.622	0.813	0.596	0.103	17.354
10	20	4.518	0.844	0.675	0.062	9.176
	30	4.429	0.883	0.665	0.081	12.137
	40	4.405	0.964	0.666	0.101	15.160
	50	4.396	0.810	0.600	0.105	17.546
12	20	5.556	0.833	0.656	0.063	9.654
	30	5.571	0.882	0.657	0.088	13.396
	40	5.503	0.980	0.659	0.109	16.508
	50	5.495	0.826	0.602	0.105	17.417

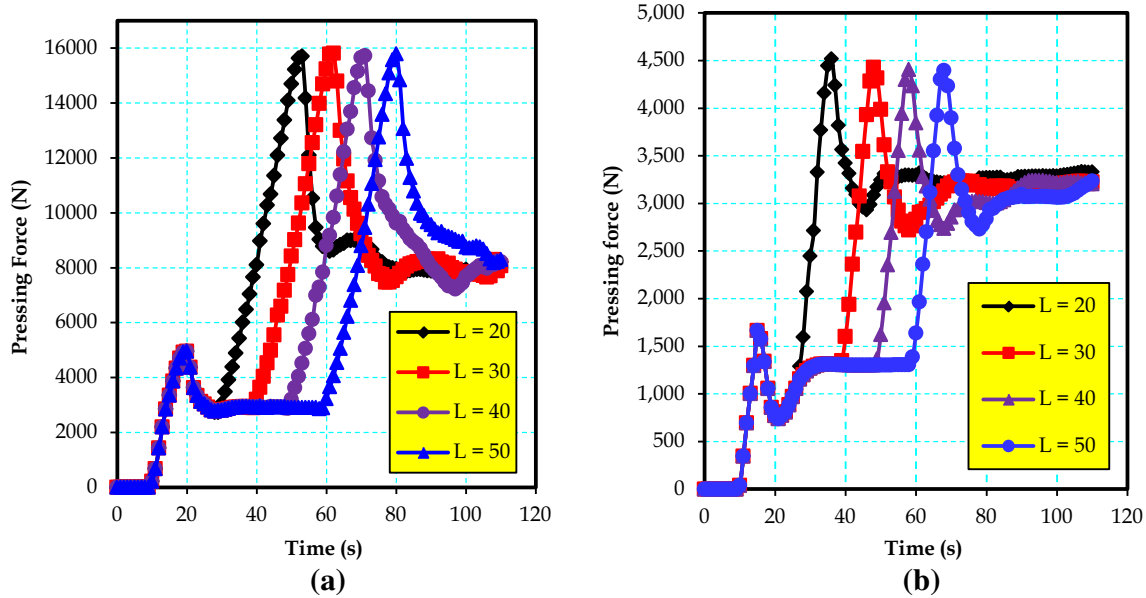


Fig. 8 Variation of pressing force required for different lengths with $t = 10$ mm in the case of: **a** 90° die and **b** 120° die

and with different lengths of the second channel. It can be seen that at the beginning of the extrusion, the pressing force starts to increase as soon as it contacts the first outer corner of the second channel. At this level, there will be initiation and growth of the shear band until the sample head crosses entirely the first elbow (the first plastic deformation zone). Then, the first plateau of the curve corresponds to the steady state of the plastic flow when the material crosses the first elbow. In addition, it can be seen that this plateau increases with the increase of the second channel length. The second stage in the pressing force will take place when the sample comes into contact with the second elbow. After it crosses the second plastic deformation zone, a second plateau with a slight undulation was observed. This can be attributed to the interaction between the plastic deformations induced by the both elbows of the die. Furthermore, it can be observed that the force required for the second pass is about 3.2 times of that required for the first pass in the case of 90° die (Fig. 8a). However, in the case of 120° die (Fig. 8b), the maximum force required for the second pass does not exceed 2.7 times of that required for the first pass. Indeed, the maximum force required for HDPE extrusion is about 16 kN in the case of 90° die and 4.5 kN in the case of 120° die. Consequently, we can say that the maximum force required in the case of 90° die is approximately 3.5 times larger than that of 120° die.

5.3 Effect of friction

In the above sections, we have assumed that the friction between the sample and the tool walls is negligible (i.e.,

frictionless condition). In this section, the friction effects on the equivalent plastic strain distribution and the pressing force are analyzed on the optimized geometries of 2-ECAP tools (with $t = 10$ mm and $L = 40$ mm for 90° and $t = 10$ mm and $L = 20$ mm for 120° die). The friction between the tool and the sample is modeled with Coulomb friction law. The computations have been performed with three friction coefficients $f = \{0.1, 0.2 \text{ and } 0.3\}$. Figure 9a, b shows, respectively, the plastic strain distribution across the sample thickness for the dies of 90° and 120°. It can be seen that the friction influences significantly the homogeneity and the magnitude of the equivalent plastic strain in the extruded material (HDPE). Indeed, more the friction coefficient increases, more is the increase of the plastic strain.

Figure 10a, b shows, respectively, the evolution of the variation factor for different friction coefficients in the case of 90° and 120° dies. It can be seen that the variation factor increases with the increase of the friction coefficient (from 0 to 0.3) in the case of 90° die. However, in the case of 120° die a slight influence of the friction on the homogeneity of the plastic strain distribution has been noticed. Consequently, to obtain a good homogeneity of the plastic strain distribution, it is advised to use a suitable lubricant in the case of 90° die, while in the case of 120° die, the extrusion can be conducted without lubricant.

To make a comparison between the behaviors of the extruded samples, the contour plots of the equivalent plastic strain distributions at different friction coefficients for 90° and 120° dies have been shown in Fig. 11, where different colors correspond to different strain magnitudes. Classical features of the ECAP process can be observed,

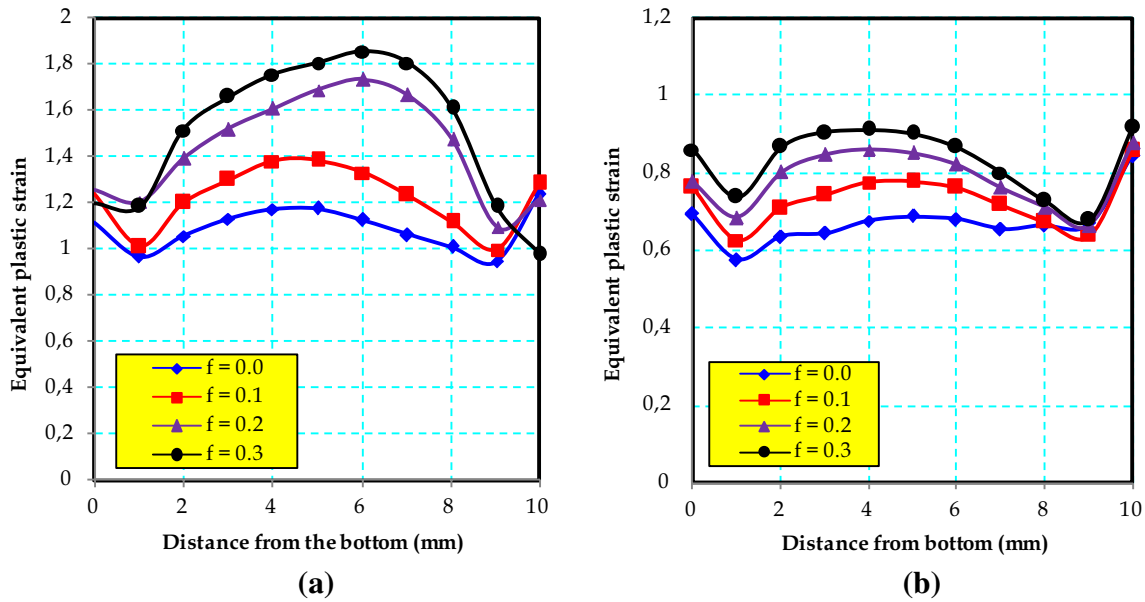
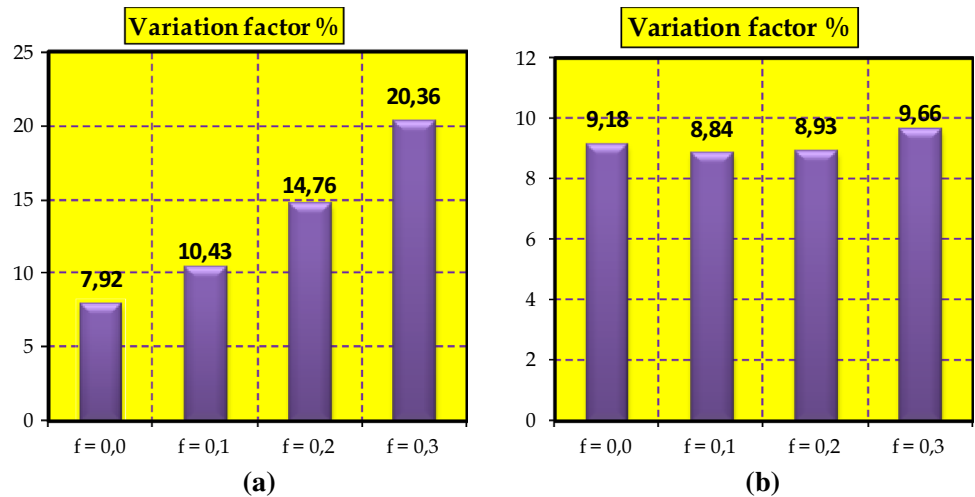


Fig. 9 Illustration of friction effect on the equivalent plastic strain distribution in the case of: a 90° die; b 120° die

Fig. 10 Illustration of friction effect on the evolution of the variation factor in the case of: a 90° die and b 120° die



such as dead zones at the corners. It can be seen that at frictionless conditions ($f = 0.0$) the corner gap at the second elbow is greater than that of the first elbow. Then, this latter starts to decrease with the increase of the friction coefficient and it vanishes at $f = 0.3$. Consequently, it is advised to reduce the maximum possible friction effect to avoid the creation of micro-cracks at the sample surfaces in contact with the die walls.

5.4 Effect of temperature

To analyze the sensitivity of the equivalent plastic strain distribution in terms of the temperature, the computations were performed for four values of $T = \{25, 40, 60$ and

$80\text{ }^\circ\text{C}\}$ at a constant ram speed of 0.1 mm/s and under frictionless conditions. The simulations are conducted using both dies with their optimized geometries ($t = 10$ mm and $L = 40$ mm for 90° die and $t = 10$ mm and $L = 20$ mm for 120° die). The distributions of the equivalent plastic strain along the sample thickness as a function of the temperature are shown in Fig. 12a for 90° die and Fig. 12b for 120° die. It can be seen that the temperature strongly influences the magnitude of the equivalent plastic strain (the higher is the temperature, the lower is the plastic strain). Furthermore, in the case of 90° die, one can notice that the distribution of the plastic strain is highly temperature sensitive at low temperatures, whereas this effect becomes insignificant beyond a certain temperature as illustrated in Fig. 12a, where the

Fig. 11 Equivalent plastic strain contours for HDPE samples during 2-ECAP for different friction coefficients in the case of: **a** 90° die and **b** 120° die

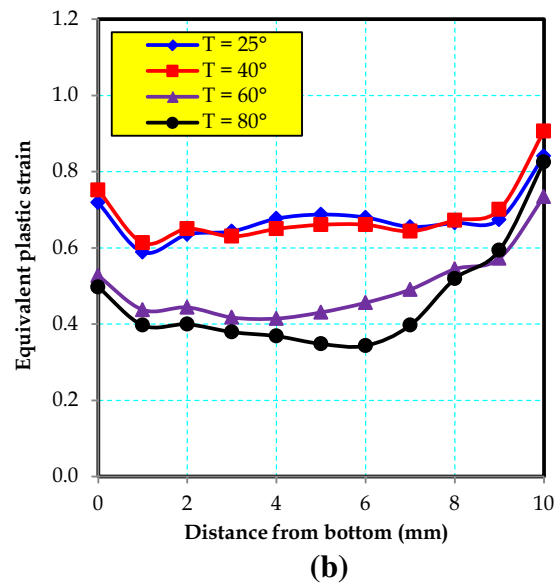
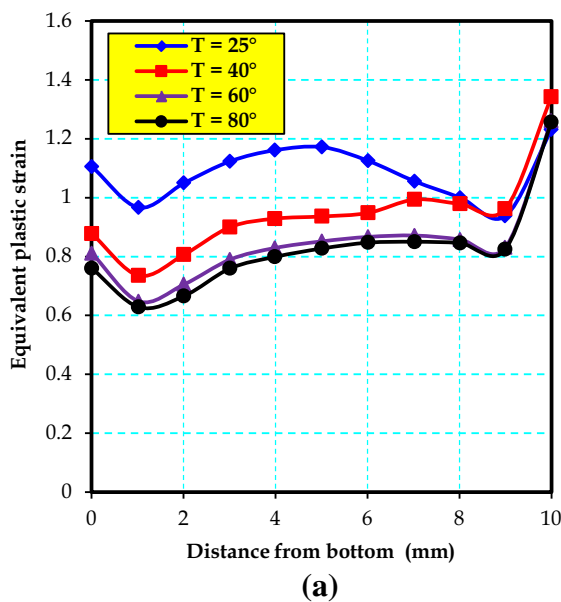
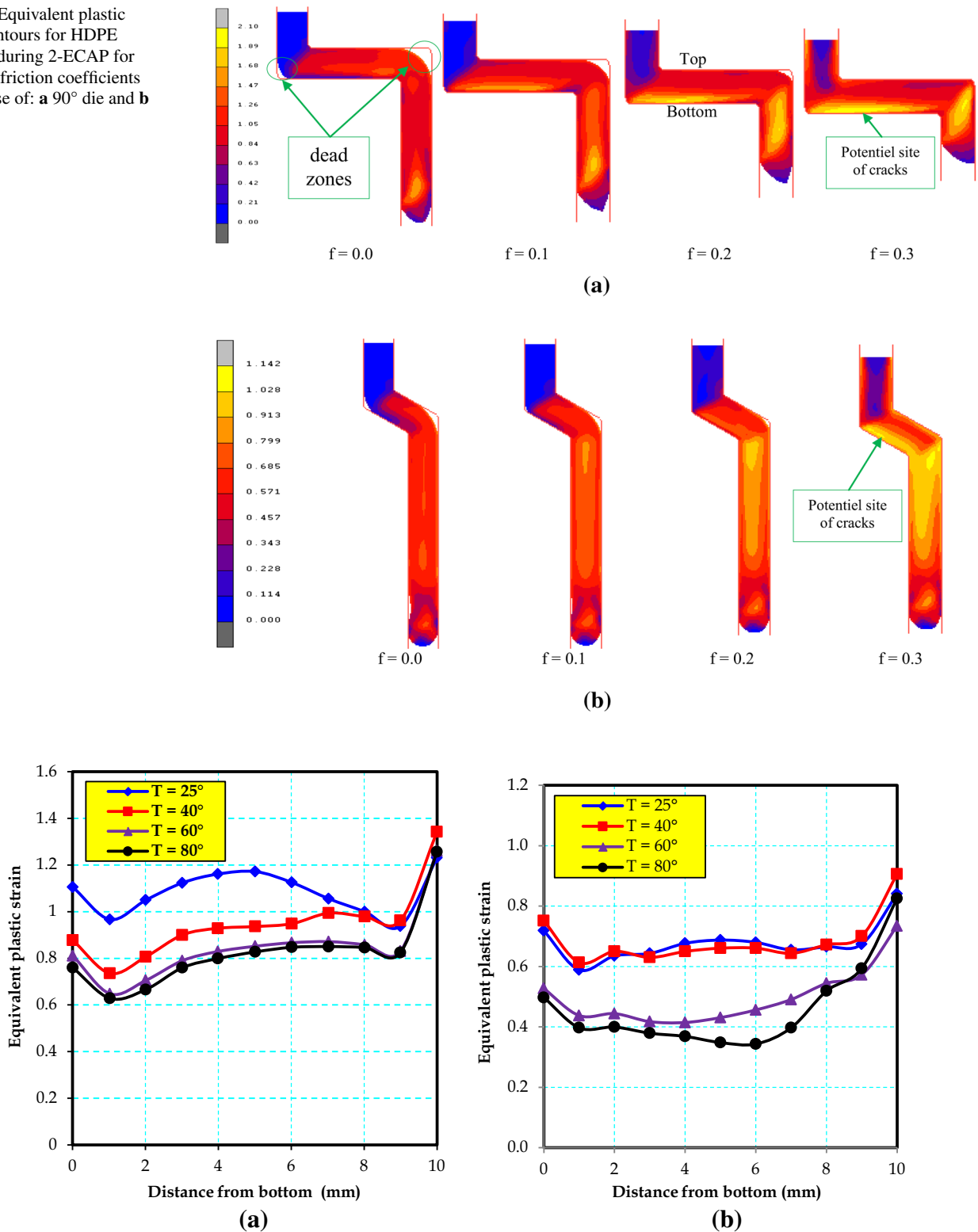


Fig. 12 Effect of the temperature on the evolution of the equivalent plastic strain in the case of: **a** 90° die and **b** 120° die

results at 60 and 80 °C are almost identical. However, in the case of 120° die, the plastic strain decreases with the increase of the temperature.

Figure 13a, b shows, respectively, the evolution of the variation factor for 90° die and 120° die. It can be observed that the variation factor increases with the increase of the

Fig. 13 Effect of the temperature on the evolution of the variation factor in the case of: **a** 90° die and **b** 120° die

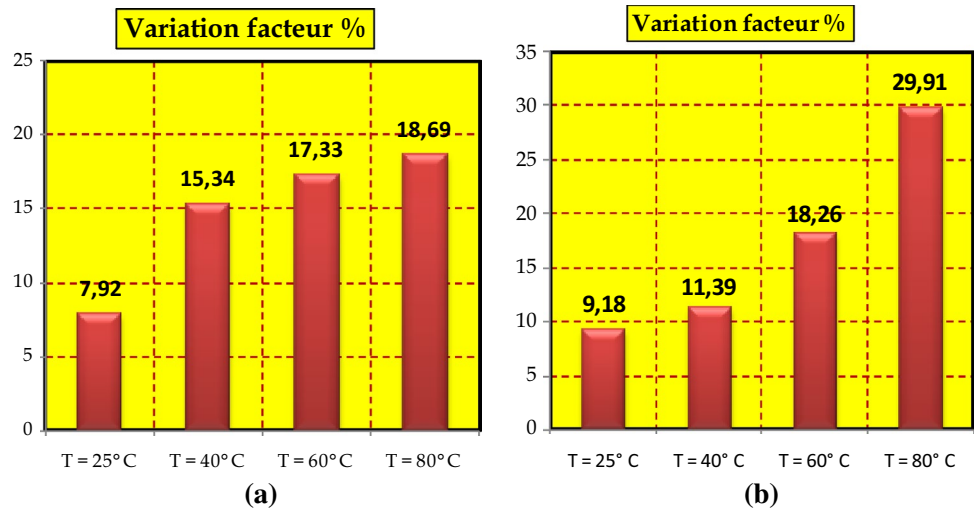
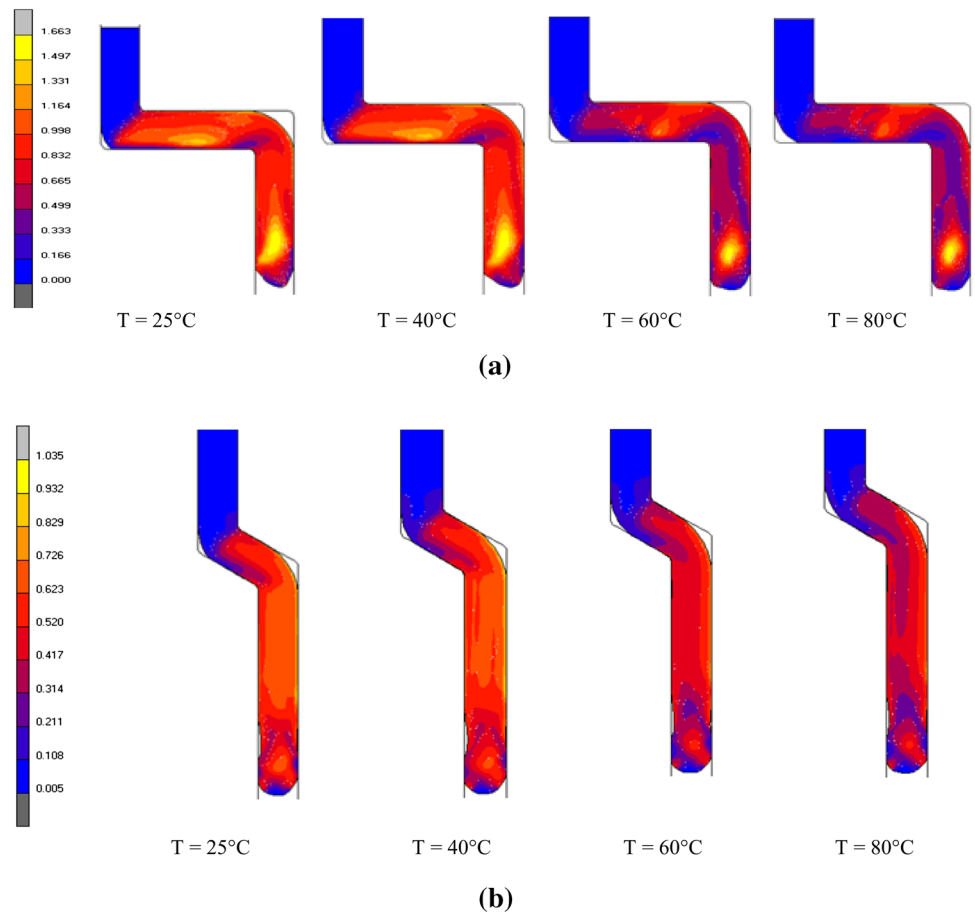


Fig. 14 Equivalent plastic strain contours for HDPE samples during 2-ECAP for different temperatures in the case of: **a** 90° die and **b** 120° die



temperature. Hence, the increase of the temperature has a negative effect on the homogeneity of the plastic strain distribution. Consequently, to obtain a high level of plastic strain with a good homogeneity, it is advised to conduct the process if possible at room temperature, else at a temperature which facilitates only the material flow during extrusion process.

The deformation behavior of the samples and the equivalent plastic strain distributions for various values of temperatures are given in Fig. 14a for 90° die and in Fig. 14b for 120° die at an intermediate level during 2-ECAP tests. It can be seen that at $T = 25$ and 40 °C the distribution of the plastic strain along the length is higher and quite homogeneous compared to that at $T = 60$ and 80 °C, especially

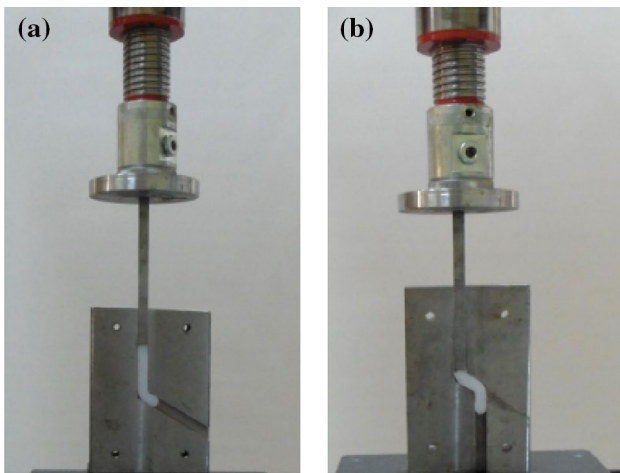


Fig. 15 Experimental study of HDPE behavior using 120 die with: **a** one elbow (1-ECAP) and **b** two elbows (2-ECAP)

in the case of 90° die. Furthermore, it can be observed that the corner gap at the first elbow is smaller than that of the second elbow and these latter increases slightly with the increase of the temperature. Indeed, the sample behavior is more affected by the increase of the temperature which allows the material to flow faster, and consequently, the level of the plastic strain will be lower.

6 Experimental tests of ECAP

After an optimization study of the geometrical parameters, a 2-ECAP device with a channel angle = 120°, a thickness $t = 10$ mm and an intermediate channel with a length $L = 20$ mm was designed and manufactured (Fig. 15a). To make a comparison between the deformed samples using 1-ECAP and 2-ECAP, another tool with one elbow and the same channel angle (=120°) was also designed and manufactured (Fig. 15b). For both dies, the lengths of the entrance and exit channels are, respectively, 85 and 80 mm. ECAP samples of 10 mm × 10 mm cross-section

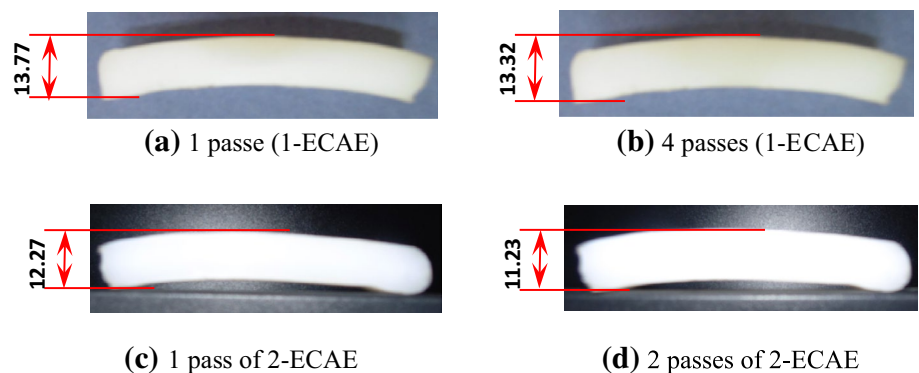
Table 4 Maximum values of the curvature of HDPE samples obtained by 1-ECAP and 2-ECAP dies with a channel angle of 120°

Type of the die	Height before extrusion, H_b (mm)	Height after extrusion, H_a (mm)	Curvature $Cu = H_a - H_b$ (mm)
1 pass (1-ECAP)	9.85	13.77	3.92
2 passes (1-ECAP)	9.85	13.28	3.43
1 pass (2-ECAP)	9.82	12.27	2.45
3 passes (1-ECAP)	9.85	13.45	3.60
4 passes (1-ECAP)	9.85	13.32	3.47
2 passes (2-ECAP)	9.82	11.23	1.41

and 70 mm in length were cut from commercially HDPE plates in the same direction, then surfaced simultaneously on the cutting facets and polished. Next, the HDPE samples were annealed in vacuum at 120 °C for 2 h. Noted that the widths and the thickness of the channels and the samples are the same, but with a clearance fit. All the ECAP tests were performed with a ram speed of 0.07 mm/s and at the room temperature of 25 °C.

The warping of the extruded samples obtained using the both dies (1-ECAP with route C and 2-ECAP) have been quantified in this experimental part. Noting that route C involves a rotation of 180° after each pass. Figure 16 shows the pictures of HDPE samples that have undergone one pass using 1-ECAP and 2-ECAP and four passes (route C) using 1-ECAP and two passes with 2-ECAP die. The obtained results for 1-ECAP and 2-ECAP are listed in Table 4 and illustrated in Fig. 16. The maximum curvature (warping) of the sample was quantified by measuring the height of the sample before and after extrusion. For a similar number of passes through the elbows, it was found that the minimum warping is always obtained using 2-ECAP die. Furthermore, the warping obtained for two passes using 2-ECAP

Fig. 16 HDPE samples extruded at room temperature after **a** one and **b** four passes using 1-ECAP die and **c** one and **d** two passes using 2-ECAP die with a channel angle of 120°



die is less than the half of that obtained using four passes with 1-ECAP die.

7 Conclusion

In the present work, the finite element method has been used to provide fruitful information for the optimization of the geometrical parameters to manufacture 2-ECAP tool which allows simultaneously an improvement of the level of the plastic strain and a significant reduction of the warping. The simulations have been performed on HDPE samples using two-turn ECAP process with channel angles of 90° and 120°. It was found that the length of the second channel, the friction and the temperature play a significant role on the homogeneity of the plastic strain distribution and the magnitude of the pressing force required for extrusion.

We noticed that the best homogeneity of the plastic strain distribution was obtained when the second channel had a thickness $t = 10$ mm and a length $L = 40$ mm in the case of 90° die, however, in the case of 120° die, the optimal dimensions are $t = 10$ mm and $L = 20$ mm.

A significant sensitivity of friction conditions on the plastic strain distribution has been found especially for 90° die. Indeed, the higher is the friction coefficient, the higher is the level of the plastic strain. So, to reduce the friction effect on the magnitude of the pressing force, it is advised to use an appropriate lubricant during the process.

The temperature of the process has also a great influence on the magnitude of the plastic strain. During 2-ECAP process, the temperature increase leads to lower plastic strain in the sample and a higher variation factor. In the particular case of HDPE samples, room temperature processing is favored, unless force limitations on the equipment require heating.

Finally, to combine the modeling analysis of the deformation behavior of HDPE samples with experimental tests, two dies with a channel angle of 120° have been designed and manufactured. The first with only one elbow, however, the second composed of two elbows according to the results of the numerical optimization. It was found that the use of two-turn ECAP tool contributes significantly on the reduction of the warping without the use of the back pressure.

References

1. Segal VM (1995) Materials processing by simple shear. *Mater Sci Eng A* 197:157–164
2. Lee S, Berbon PB, Furukawa M, Horita Z, Nemoto M, Tsenev NK, Valiev RZ, Langdon TG (1999) Developing superplastic properties in an aluminum alloy through severe plastic deformation. *Mater Sci Eng A* 272:63–72
3. Beyerlein IJ, Tomé CN (2004) Analytical modeling of material flow in equal channel angular extrusion (ECAE). *Mater Sci Eng A* 380:171–190
4. Kim HS, Estrin Y (2005) Microstructural modelling of equal channel angular pressing for producing ultrafine grained materials. *Mater Sci Eng A* 410–411:285–289
5. Sue HJ, Li CKY (1998) Control of orientation of lamellar structure in linear low density polyethylene via a novel equal channel angular extrusion process. *J Mater Sci Lett* 17:853–856
6. Sue HJ, Dilan H, Li CKY (1999) Simple shear plastic deformation behavior of polycarbonate plate due to the equal channel angular extrusion process. I: Finite element methods modelling. *Polym Eng Sci* 39:2505–2515
7. Li CKY, Xia ZY, Sue HJ (2000) Simple shear plastic deformation behavior of polycarbonate plate. II: Mechanical property characterization. *Polymer* 41:6285–6293
8. Xia Z, Sue HJ, Hsieh AJ (2001) Impact fracture behavior of molecularly orientated polycarbonate sheets. *J Appl Polym Sci* 79:2060–2066
9. Xia Z, Sue HJ, Hsieh AJ, Huang JWL (2001) Dynamic mechanical behavior of oriented semi-crystalline polyethylene terephthalate. *J Polym Sci Part B Polym Phys* 39:1394–1403
10. Creasy TS, Kang YS (2005) Fiber fracture during equal-channel angular extrusion of short fiber-reinforced thermoplastics. *J Mater Process Technol* 160:90–98
11. Weon JI, Creasy TS, Sue HJ, Hsieh AJ (2005) Mechanical behavior of polymethyl-methacrylate with molecules oriented via simple shear. *Polym Eng Sci* 45:314–324
12. Weon JI, Sue HJ (2005) Effects of clay orientation and aspect ratio on mechanical behavior of nylon-6 nanocomposites. *Polymer* 46:6325–6334
13. Wang ZG, Xia ZY, Yu ZQ, Chen EQ, Sue HJ, Han CC, Hsiao BS (2006) Lamellar formation and relaxation in simple sheared poly(ethylene terephthalate) by small-angle X-ray scattering. *Macromolecules* 39:2930–2939
14. Zaïri F, Aour B, Gloaguen JM, Naït-Abdelaziz M, Lefebvre JM (2008) Steady plastic flow of a polymer during ECAE process: experiments and numerical modeling. *Polym Eng Sci* 18:1015–1021
15. Aour B, Zaïri F, Gloaguen JM, Naït-Abdelaziz M, Lefebvre JM (2009) Finite element analysis of plastic strain distribution in multi-pass ECAE process of high density polyethylene. *J Manuf Sci E* 131(0310161):1–11
16. Bouaksa F, Ovalle Rodas C, Zaïri F, Stoclet G, Naït-Abdelaziz M, Gloaguen JM, Tamine T, Lefebvre JM (2014) Molecular chain orientation in polycarbonate during equal channel angular extrusion: experiments and simulations. *Comput Mater Sci* 85:244–252
17. Li CKY, Xia ZY, Sue HJ (2000) Simple shear plastic deformation behavior of polycarbonate plate. II: Mechanical property characterization. *Polymer* 41:6285–6293
18. Tervoort TA, Smit RJM, Brekelmans WAM, Govaert L (1998) A constitutive equation for the elasto-viscoplastic deformation of glassy polymers. *Mech Time Depend Mater* 1:269–291
19. Boyce MC, Socrate S, Llana PG (2000) Constitutive model for the finite deformation stress-strain behavior of poly(ethylene terephthalate) above the glass transition. *Polymers* 41:2183–2201
20. Aour B, Zaïri F, Gloaguen JM, Naït-Abdelaziz M, Lefebvre JM (2009) Finite element analysis of plastic strain distribution in multi-pass ECAE process of high density polyethylene. *J Manuf Sci E* 131(0310161):1–11
21. Aour B, Zaïri F, Gloaguen JM, Naït-Abdelaziz M, Lefebvre JM (2006) Numerical investigation on equal channel angular extrusion process of polymers. *Comput Mater Sci* 37:491–506
22. Aour B, Zaïri F, Gloaguen JM, Naït-Abdelaziz M, Lefebvre JM (2008) A computational study of die geometry and processing

- conditions effects on equal channel angular extrusion of a polymer. *Int J Mech Sci* 50:589–602
23. Taheri S, Lorentz E (1997) An elastoplastic constitutive law for description of uniaxial and multiaxial ratchetting. *Plasticity* 97, Alaska
 24. Taheri S (2005) *Le Faïençage thermique à grand nombre de cycles*. HDR, Université Paris XIII, France
 25. Yamaguchi D, Horita Z, Nemoto M, Langdon TG (1999) Significance of adiabatic heating in equal-channel angular pressing. *Scr Mater* 41:791–796